Supporting Information

Facile construction of $CuFe_2O_4$/g-C_3N_4 photocatalyst for enhanced visible-light hydrogen evolution

*Ruolin Cheng, Xiangqian Fan, Min Wang, Mengli Li, JianjianTian, Lingxia Zhang**

State Key Laboratory of High Performance Ceramics and Superfine Microstruture, Shanghai Institute of Ceramics, Chinese Academy of Sciences, 1295 Ding-xi Road, Shanghai 200050 (P. R. China)

Correspondence to:

E-mail: zhlingxia@mail.sic.ac.cn (L.X. Zhang)

Supplementary Figures and Tables

Table S1. Cu, Fecontent of the as-prepared CN and xCuFe-CN samples

Sample	CN	1CuFe-CN	3CuFe-CN	5CuFe-CN	10CuFe-CN	30CuFe-CN
Cu/ wt%	/	0.02	0.10	0.13	0.22	0.69
Fe/ wt%	/	0.05	0.19	0.23	0.45	1.24
$g\text{-}C_3N_4$/wt%	100	99.9	99.7	99.6	99.3	98.1
[a]Yield /g	0.9	0.76	0.72	0.71	0.69	0.61
[a]Net amount of $g\text{-}C_3N_4$/ g	0.9	0.76	0.72	0.71	0.69	0.60

[a] Yield of samples and the net amount of $g\text{-}C_3N_4$ in the samples obtained from 20 g urea and x mg $CuFe_2O_4$ precursor

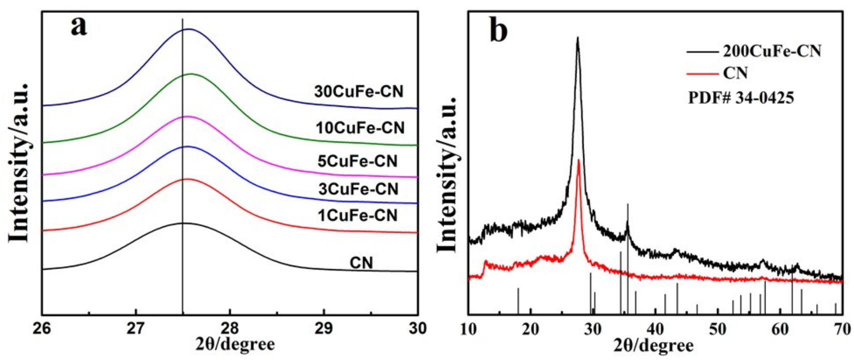

Figure S1. (a) Enlarged XRD patterns of xCuFe-CN composite with different mass fraction; (b) XRD patterns of CN and 200CuFe-CN.

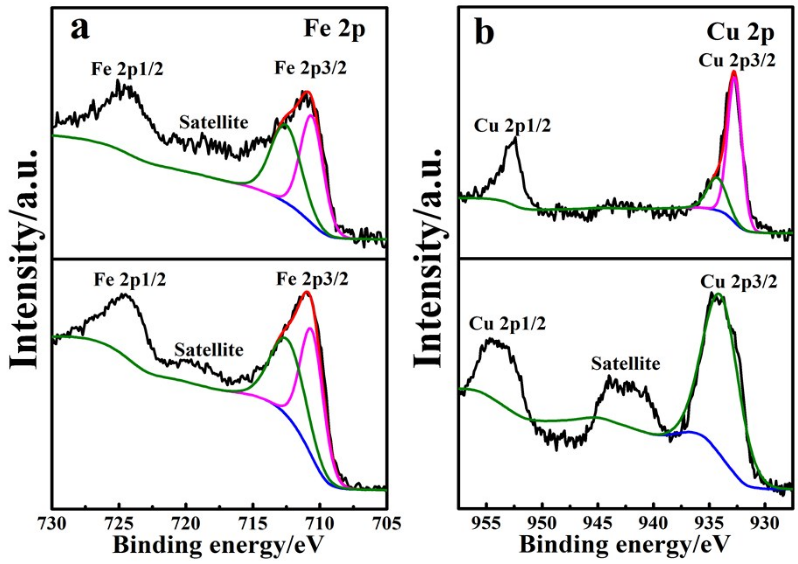

Figure S2. XPS spectra of CuFe and 200CuFe-CN:(a) Fe 2p, (b) Cu 2p spectra.

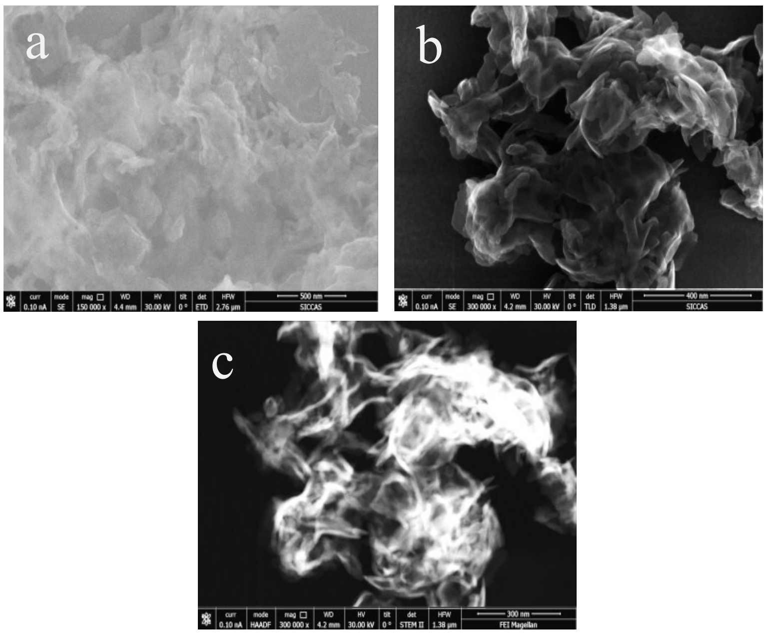

Figure S3. Typical SEM images of (a) CN and (b) 3CuFe-CN, (c) STEM image of 3CuFe-CN.

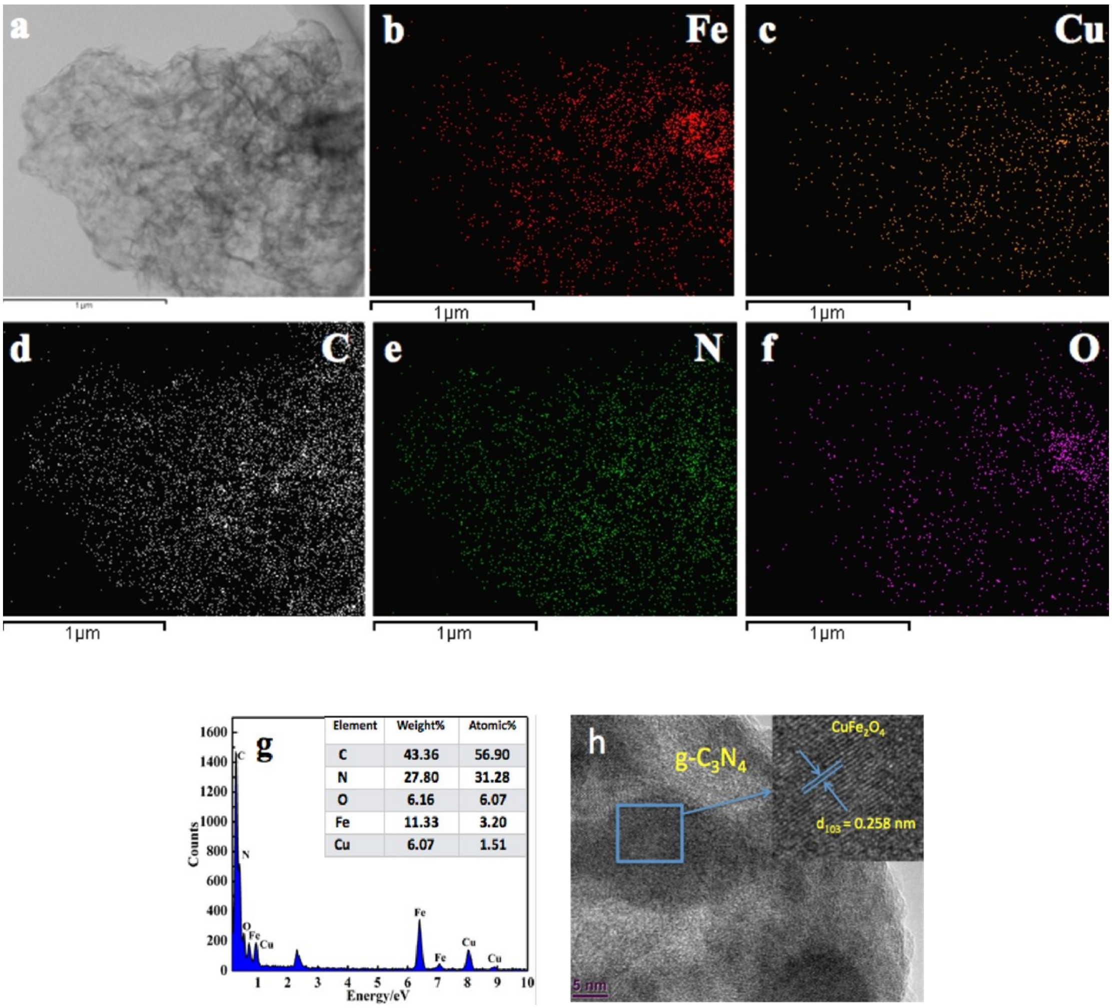

Figure S4. STEM (a) and the corresponding element mappings (b–f) and the EDX spectrum, (h) HRTEM image of 200CuFe-CN.

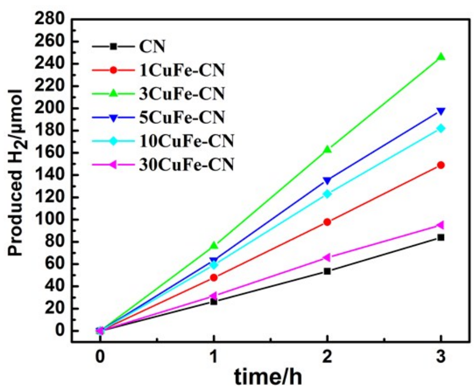

Figure S5. Photocatalytic H_2 evolution on pure CN and xCuFe-CN composite under visible light irradiation (λ> 420 nm).

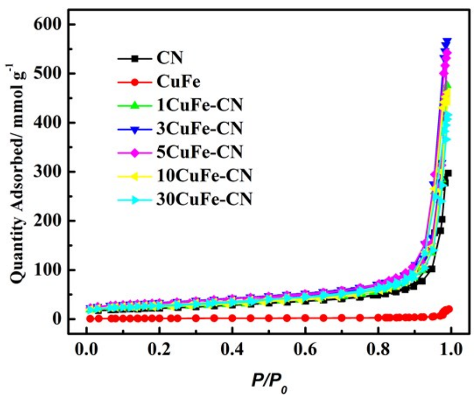

Figure S6. N_2 adsorption-desorption isotherms of CN, CuFe and xCuFe-CN composite.

Table S2. Summary of bandgap results of CN, CuFe and xCuFe-CN composite

Sample	CN	CuFe	1CuFe-CN	3CuFe-CN	5CuFe-CN	10CuFe-CN	30CuFe-CN
Bandgap/eV	2.89	1.42	2.88	2.86	2.85	2.83	2.82

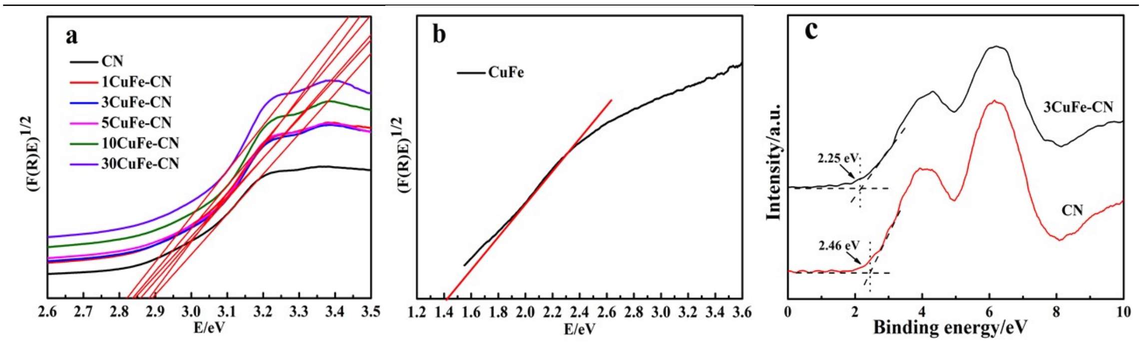

Figure S7. The Tauc plots of CN and xCuFe-CN samples (a), and CuFe (b). Each bandgap is determined by the intersection point of the corresponding tangent line and horizontal axis. Valence band XPS spectra of traditional CN and 3CuFe-CN (c).

The Kubelka–Munk method was used to determine the bandgaps of CN, CuFe and all the modified samples. The intrinsic HOMO energy levels of CN and 3CuFe-CN were analysed by performing the valence band X-ray photoelectron spectroscopy.